JOMH
Journal of Men's Health

ORIGINAL RESEARCH

Liquid chromatography-mass spectrometry-based metabolic panels characteristic for patients with prostate cancer and prostate-specific antigen levels of 4–10 ng/mL

Chen Wang[1], Ting Chen[1], Teng-Fei Gu[1], Sheng-Ping Hu[1], Yong-Tao Pan[1], Jie Li[1],*

[1]Department of Urology, Lishui Municipal Central Hospital, 323000 Lishui, Zhejiang, China

*Correspondence
lijie9783@wmu.edu.cn
(Jie Li)

Abstract

Background: Prostate cancer is the second most common malignant tumor among men worldwide. This study explores potential metabolic biomarkers and pathways through metabolomics and evaluates the diagnostic performance of a metabolic panel in distinguishing prostate cancer, benign prostatic hyperplasia (BPH) and prostatitis. **Methods**: Liquid chromatography-mass spectrometry (LC-MS) was used to perform untargeted metabolomic analysis on serum samples from 30 prostate cancer patients, 30 BPH patients, and 30 prostatitis patients. Based on the identified metabolites, LASSO regression was applied for variable selection, and logistic regression and support vector machine models were developed. **Results**: The LASSO algorithm's ability to select variables effectively reduced redundant features and minimized model overfitting. Receiver Operating Characteristic (ROC) analysis demonstrated strong diagnostic performance, with an area under the curve of 0.852 for prostate cancer versus BPH and 0.891 for prostate cancer versus prostatitis. Enrichment analysis revealed that fatty acid metabolism, particularly the biosynthesis of unsaturated fatty acids, is a key metabolic feature of prostate cancer. **Conclusions**: This study demonstrates that metabolites selected through the LASSO algorithm, combined with machine learning models, enhance the early diagnosis of prostate cancer and exhibit excellent performance in distinguishing it from BPH and prostatitis. These findings lay a foundation for precision medicine and disease screening, with potential applications in early intervention and personalized treatment in clinical practice.

Keywords

Prostate cancer; Metabolomics; LASSO regression; Machine learning models; Fatty acid metabolism

1. Introduction

Prostate cancer (PCa) is the second leading cause of cancer-related deaths among men, and its incidence has been steadily increasing worldwide, posing a significant public health challenge [1, 2]. Currently, prostate-specific antigen (PSA) is the most widely used biomarker for PCa screening and diagnosis [3]. However, while PSA is organ-specific, it is not cancer-specific, as elevated PSA levels can also occur in patients with benign prostatic hyperplasia (BPH) or prostatitis, reducing its diagnostic precision. Even with the use of complementary clinical parameters—such as PSA density, free-to-total PSA ratio, or multiparametric magnetic resonance imaging (mpMRI)—distinguishing PCa from other benign conditions remains challenging. This difficulty is particularly evident when PSA levels fall within the 4–10 ng/mL "gray zone", where the positive biopsy rate is only 25–40%, resulting in unnecessary biopsies and increased healthcare burdens [4, 5].

Thus, novel biomarkers are urgently needed to improve the accuracy of early PCa detection and reduce the frequency of unnecessary invasive procedures.

In recent years, metabolomics has gained attention as a powerful, high-throughput approach for identifying metabolic alterations associated with diseases [6]. By analyzing small-molecule metabolites in biofluids such as blood and urine, metabolomics offers insights into the metabolic disruptions involved in disease onset and progression, providing potential biomarkers for clinical diagnosis [7, 8]. Compared to urinary metabolomics, serum metabolomics has several advantages: it eliminates the need for prostate massage, reducing patient discomfort and operational complexity [9]. Additionally, as a noninvasive and convenient screening tool, serum metabolomics is well-suited for large-scale population studies [8].

While previous studies have employed nuclear magnetic

resonance (NMR) or gas chromatography-mass spectrometry (GC-MS) to investigate metabolic changes in PCa, these methods have limitations. NMR lacks sensitivity, and GC-MS can only detect small volatile compounds [10]. In contrast, liquid chromatography-mass spectrometry (LC-MS) offers higher sensitivity and can identify larger, thermally unstable metabolites, providing a more comprehensive metabolic profile [11, 12].

For example, Bondar *et al.* [13] (2007) used LC-MS/MS to measure serum levels of Zn-α2-glycoprotein (ZAG), finding that ZAG levels were significantly higher in PCa patients (7.59 mg/L) than in BPH patients (6.21 mg/L) and healthy individuals (3.65 mg/L, $p = 0.0007$). These results suggest that ZAG can help differentiate malignant from benign conditions. However, the study was limited by a small sample size and reliance on a single biomarker, and ZAG levels were found to be influenced by other metabolic disorders [13]. Therefore, multi-biomarker approaches are necessary to improve diagnostic accuracy and ensure reliable predictions.

This study aims to systematically analyze the serum metabolic profiles of patients with PCa, BPH and prostatitis using LC-MS [13] to identify biomarkers that can accurately distinguish PCa from other benign prostate diseases. We hypothesize that the metabolic profiles of PCa patients differ significantly from those of BPH and prostatitis patients and that LC-MS analysis can effectively distinguish between these three conditions. Furthermore, we will apply machine learning algorithms to the selected metabolites to enhance diagnostic performance, especially when PSA levels fall within the 4–10 ng/mL gray zone. By integrating metabolomics with machine learning, we aim to develop a novel noninvasive diagnostic tool for early PCa detection, reducing unnecessary biopsies, improving diagnostic efficiency, and supporting precision medicine. Ultimately, this approach seeks to enhance patient outcomes, survival rates, and quality of life.

2. Materials and methods

2.1 Study participants

In this retrospective cross-sectional study, we analyzed the data of 90 participants—30 patients with PCa, 30 with BPH, and 30 with prostatitis—who were admitted to Lishui Central Hospital (the Fifth Affiliated Hospital of Wenzhou Medical College) between August 2021 and December 2023. All participants underwent PSA screening, biopsy, transrectal ultrasound (TRUS), and digital rectal examination (DRE) following the National Comprehensive Cancer Network guidelines for PCa [14]. Written informed consent was obtained from all participants prior to their inclusion in the study. All participants were enrolled by a urologist based on clinical criteria for diagnosing BPH, prostatitis and PCa. PSA levels for all participants ranged 4–10 ng/mL. Prostate cancer was defined as follows: (i) nodules detected through DRE; (ii) hyper- or hypoechoic lesions seen in TRUS; and (iii) biopsy-confirmed PCa with a Gleason score of 6 or above. BPH was diagnosed after a negative DRE, TRUS and biopsy result. The diagnosis of prostatitis had to meet one of the following criteria: (1) infiltration of inflammatory cells within the prostate stroma or (2) infiltration of inflammatory cells in the area surrounding the prostate [15], with the infiltrate primarily comprising lymphocytes, along with plasma cells.

Participants were eligible for inclusion if they were above 50 years of age, had PSA levels between 4 and 10 ng/mL, and had not used 5α-reductase inhibitors or other medications affecting PSA levels in the past year. Additional criteria included no prior prostate biopsy, no previous diagnosis of PCa, no acute urinary tract infection or indwelling catheter within the past 2 weeks, and completion of mpMRI within 2 weeks of the prostate biopsy. Moreover, participants had to be willing to provide blood samples and sign written informed consent. Exclusion criteria included a history of other cancers, severe cardiovascular, hepatic, or renal diseases, psychiatric disorders, use of 5α-reductase inhibitors (*e.g.*, finasteride) for more than three months, incomplete clinical records, or refusal to sign the informed consent.

2.2 Materials and reagents

Fisher Scientific (Fair Lawn, NJ, USA) supplied acetonitrile, methanol, and formic acid (LC-MS grade). Sigma-Aldrich (St. Louis, MO, USA) provided ammonium bicarbonate (LC-MS grade). Internal standards were furnished by Cambridge Isotope Laboratories, Inc. (Tewksbury, MA, USA), Toronto Research Chemicals (Toronto, Canada), and Avanti Polar Lipid, Inc. (Birmingham, AL, USA). The ultrapure water was generated using the Milli-Q water system (Merck KGaA, Darmstadt, Germany).

2.3 Sample collection and preparation

Following the standard operating procedure, blood samples and clinical characteristics were collected from participants. All participants fasted overnight, and their blood was drawn the next morning. To ensure complete coagulation, the samples were transferred into serum gel tubes, gently inverted five times, and left at room temperature for 60 minutes. The samples were then centrifuged at 4 °C for 10 minutes at 1500g to separate serum, which was aliquoted into cryovials and stored at −80 °C.

Polar metabolites from each serum sample were extracted and analyzed using two detection methods, both employing reverse-phase chromatography: technique 1 used positive ionization mode, while technique 2 used negative ionization mode. After thawing the samples at 4 °C, 100 μL of each sample was mixed with 400 μL of a methanol-acetonitrile solution containing isotope-labeled internal standards (ISs). The internal standards included: chenodeoxycholic acid-d4 (1.0 μg/mL), AcCa(12:0)-d9 (0.2 μg/mL), AcCa(18:0)-d3 (0.2 μg/mL), palmitic acid-13C16 (0.2 μg/mL), hippuric acid-d5 (1.0 μg/mL), stearic acid-d35 (1.0 μg/mL), Chlorophenylalanine (1.0 μg/mL), and taurine-d4 (1.0 μg/mL). The mixture was vortexed for 5 minutes and centrifuged at 13,000g for 15 minutes at 4 °C. Two 200 μL aliquots of the supernatant were transferred to a CentriVap concentrator (centrifugal vacuum concentrator, Labconco Corporation, Kansas, MO, USA) and freeze-dried. The quality of sample preparation was assessed by calculating the relative standard deviation (RSD%) of the raw mass spectrometry

response values of the internal standards across all samples, with results ranging from 1.07% to 16.37%, meeting the technical requirements for biological sample analysis. Equal portions of each sample extract were pooled to serve as analytical quality control (QC) samples, and all samples were prepared in parallel for testing.

To ensure analytical integrity, four QC samples were evenly distributed at the beginning, middle, and end of each data collection sequence. Quality control results were assessed using principal component analysis (PCA), time-series plotting of the first principal component, and Spearman correlation analysis between the initial and final QC samples. To rehydrate the freeze-dried samples, 120 μL of a 1:1 methanol/water solution was added to each sample.

2.4 Ultra-high-performance liquid chromatography high-resolution mass spectrometry (UHPLC-HRMS) analytical methods

An Ultimate™ 3000 UPLC system coupled with a Q Exactive™ Quadrupole-Orbitrap mass spectrometer (Thermo Scientific, San Jose, CA, USA) was used in the measurements of the metabolites. In method 1, metabolites were separated by an ACE C18-PFP column and then detected using positive electrospray. As mobile phases, water (A) and acetonitrile (B) with 0.1% formic acid were used. Over a period of 10 minutes, the linear gradient increased from 2% to 98% organic mobile phase. For method 2, the metabolome was analyzed in negative ion mode using an Acquity™ HSS C18 column provided by Waters Corporation (Milford, USA). A mixture of water and acetonitrile/methanol with 5 mM ammonium bicarbonate (NH_4HCO_3) was utilized as the mobile phase. A gradient was established to start at 2% organic phase, ramping up to 100% over 10 minutes, followed by an additional 5 minutes for column washing and equilibration. Both methods used the same flow rate (0.4 mL/min), injection volume (5 μL), and column temperature (50 °C).

Quadrupole-Orbitrap mass spectrometers functioned with identical ionization parameters except for the ionization voltage, using heated electrospray ionization (ESI) sources. The parameters included sheath gas at 45 arbitrary units (arb), auxiliary gas at 10 arb, heater temperature at 355 °C, capillary temperature at 320 °C, and S-Lens RF level at 55%. Using Automatic Gain Control (AGC) set to 1E6 and a max injection time of 200 ms, 70,000 full widths at half maximum resolution were applied to metabolome extracts in full scan mode. The scan range was 70–1000 m/z. QC samples were repeatedly injected to obtain the top 10 data-dependent MS2 spectra (full scan-ddMS2) for detailed metabolite structural annotation. A resolution setting of 17,500 Full Width at Half Maximum (FWHM) was used for the acquisition of full MS/MS data. Stepped normalized collision energy was used for the collision-induced dissociation of metabolites, with ultrapure nitrogen serving as the fragmentation gas.

2.5 Metabolomic data processing

Metabolic peaks were processed for component extraction using Compound Discoverer 2.1 software (Thermo Scientific, San Jose, CA, USA). Structural annotation was further achieved by comparing the acquired MS2 data with the proprietary iPhenome™ SMOL high-resolution MS/MS spectrum local library, generated with the mzCloud library, as well as authentic standards. Additionally, exact m/z values (± 5 ppm) from MS1 spectra were matched against the Chemical metabolite database based on the Human Metabolome Database (HMDB) [16]. Separate manual inspections of the proposed identification results were required to eliminate false positives. The metabolomic data were normalized, trimmed, and log-transformed for further processing [17]. SIMCA-P software (version 14.1, Sartorius AG Umetrics, Goettingen, NI, Germany), which comprises orthogonal partial least squares discriminant analysis (OPLS-DA) and PCA, was used for multivariate analyses. Additionally, univariate analyses, such as independent sample t-tests and false discovery rate adjustments using the Benjamini-Hochberg method, as well as data visualization and Chemical Similarity Enrichment Analysis (ChemRICH) chemical enrichment analysis, were conducted on a proprietary R-based cloud computing platform, Integrated Pathway-Oriented Scoring (IPOS) [18]. Metabolic pathway analysis of differential metabolites was executed by the MetaboAnalyst platform, and metabolite-metabolite interaction networks were constructed [19].

2.6 LASSO feature selection and cross-validation for prostate cancer classification

We performed 5-fold cross-validation on two classification tasks: distinguishing between PCa and BPH and between prostate cancer and prostatitis. First, using differential metabolites as features, we applied LASSO regression for feature selection, incorporating L1 regularization to reduce redundant features and minimize the risk of overfitting. Additionally, we selected differential metabolites with an area under the curve (AUC) greater than 0.7 as input features. Next, in K-fold cross-validation, we trained and compared the performance of Support Vector Machine (SVM) and logistic regression models, evaluating metrics such as accuracy, precision, recall, F1-score, and receiving operating characteristic (ROC)-AUC. Finally, based on the cross-validation results, we selected the best-performing model and retrained it on the entire dataset filtered by LASSO to ensure robust prediction accuracy and generalizability in real-world applications.

2.7 Statistical analysis

Figures were created using R software 4.2.2 (R Foundation for Statistical Computing, Vienna, Austria; available at http://www.R-project.org). Statistical significance was set at $p < 0.05$ or an adjusted $p < 0.05$. Differences between the two groups were evaluated using the non-parametric Mann-Whitney U test and the parametric Student's t-test. The adjusted p-value was calculated using the Benjamini-Hochberg correction, and categorical variables were assessed using the chi-square test.

3. Results

3.1 Clinical characteristics of the study participants

The clinical features of the 90 enrolled patients are summarized in Table 1. No significant differences were observed in age or PSA levels among the three clusters. However, significant differences were found in the ratio of free PSA to total PSA, prostate volume, PSA density, Prostate Imaging-Reporting and Data System (PI-RADS) score, and the proportion of positive findings from digital rectal examination (DRE), ultrasonography, and contrast-enhanced ultrasonography (Table 1). Specifically, the ratio of free-to-total PSA and prostate volume was lower in PCa patients than in those with prostatitis or BPH. In contrast, PSA density and PI-RADS scores were higher in PCa patients than in those with BPH or prostatitis. Additionally, the proportion of patients with positive findings from DRE, ultrasonography, or contrast-enhanced ultrasonography was higher in the PCa group compared to those with BPH or prostatitis.

3.2 Quality control

Analytical quality control was maintained using a pooled QC strategy. In the PCA, the QC samples clustered tightly (Fig. 1), indicating the experimental platform's stable performance throughout the analytical process and the reliability of the test data. Additionally, the minimal variation in principal component 1 (PC1) for the QC samples further confirmed the stability of the analysis (Fig. 2). Spearman's correlation analysis was performed between the first and last QC data matrices, with the results shown in a Spearman correlation scatter plot (Fig. 3). Although the correlation coefficients were smallest between these two groups of QC samples, the lowest correlation was still 0.998, highlighting the excellent data quality. Furthermore, isotope-labeled internal standards were added to the extracts, and sample pretreatment was evaluated by the RSD% of the raw mass spectral response of the internal standards in each sample. The RSD% ranged from 1.07% to 16.37%, which meets the technical requirements for biological sample analyses.

3.3 Metabolomic profiling differences between PCa and BPH

PCA analysis showed no significant differences in the metabolic profiles between PCa and benign prostatic hyperplasia (BPH) (Fig. 4A). However, the OPLS-DA score scatter plot clearly distinguished PCa from BPH (Fig. 4B), with R^2Y and Q^2 values of 0.728 and 0.0138, respectively, indicating the model's reliability. Through OPLS-DA, metabolites with Variable Importance in Projection (VIP) scores greater than 1.0 and p-values less than 0.05 were identified as differential metabolites. After excluding exogenous metabolites, 12 key metabolites that distinguish PCa from BPH were identified using the LASSO regression algorithm (Table 2), with six detected in ESI+ mode and six in

TABLE 1. Clinical characteristics of the study population.

Variable	Overall, N = 90[1]	Classification of diseases			p-value[2]
		PCa N = 30 (33%)[1]	Prostatitis N = 30 (33%)[1]	BPH N = 30 (33%)[1]	
Age (yr)	69.50 (7.14)	69.30 (7.82)	69.93 (8.17)	69.27 (5.32)	0.922
tPSA (ng/mL)	5.65 [4.46, 6.99]	6.12 [4.83, 7.21]	5.52 [4.55, 6.98]	4.77 [4.37, 6.93]	0.377
f/tPSA	0.21 [0.16, 0.26]	0.17 [0.11, 0.23]	0.22 [0.15, 0.28]	0.22 [0.19, 0.28]	0.018
PV (cm^3)	39.97 [28.04, 52.68]	30.45 [22.15, 41.80]	43.00 [32.28, 53.91]	46.15 [36.27, 57.00]	0.005
PSAD	0.14 [0.11, 0.20]	0.21 [0.13, 0.26]	0.14 [0.11, 0.17]	0.12 [0.10, 0.14]	0.001
PI-RADS	3.00 [2.00, 4.00]	4.00 [3.00, 4.00]	3.00 [2.00, 4.00]	3.00 [2.00, 4.00]	0.006
DRE					
Negative	66 (73.33%)	16 (53.33%)	25 (83.33%)	25 (83.33%)	0.010
Positive	24 (26.67%)	14 (46.67%)	5 (16.67%)	5 (16.67%)	
Ultrasonography					
Negative	55 (61.11%)	12 (40.00%)	17 (56.67%)	26 (86.67%)	0.001
Positive	35 (38.89%)	18 (60.00%)	13 (43.33%)	4 (13.33%)	
CEUS					
Negative	46 (51.11%)	9 (30.00%)	13 (43.33%)	24 (80.00%)	0.001
Positive	44 (48.89%)	21 (70.00%)	17 (56.67%)	6 (20.00%)	

[1] Mean (SD); Median [IQR]; n (%); [2] One-way ANOVA; Kruskal-Wallis rank sum test; Pearson's Chi-squared test; Fisher's exact test.

Abbreviations: BPH, benign prostatic hyperplasia; CEUS, contrast-enhanced ultrasonography; DRE, digital rectal examination; f/tPSA, ratio of free-to-total PSA; IQR, interquartile range; PCa, prostate cancer; PI-RADS, prostate imaging reporting and data system; PSAD, PSA density; PV, prostate volume; SD, standard deviation; tPSA, total prostate-specific antigen.
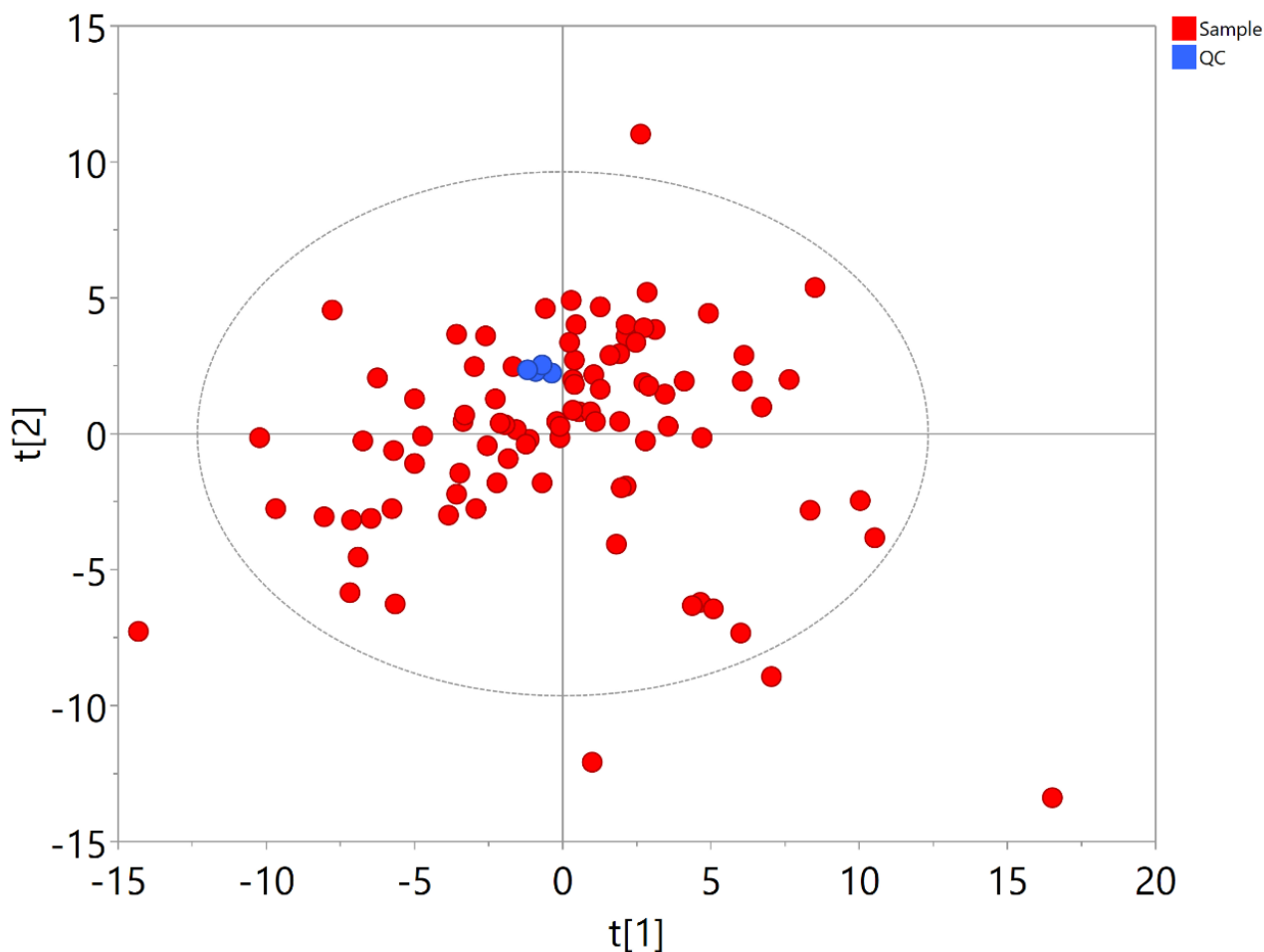
F I G U R E 1. QC samples clustered tightly in the unsupervised PCA score plot, indicating stable analytical performance throughout the batch and confirming the high quality of the metabolomic data. Blue dots: QC pooled batch QC samples; red dots: samples tested in this project. Pareto scaling for PCA. PCA, principal component analysis; QC, quality control.
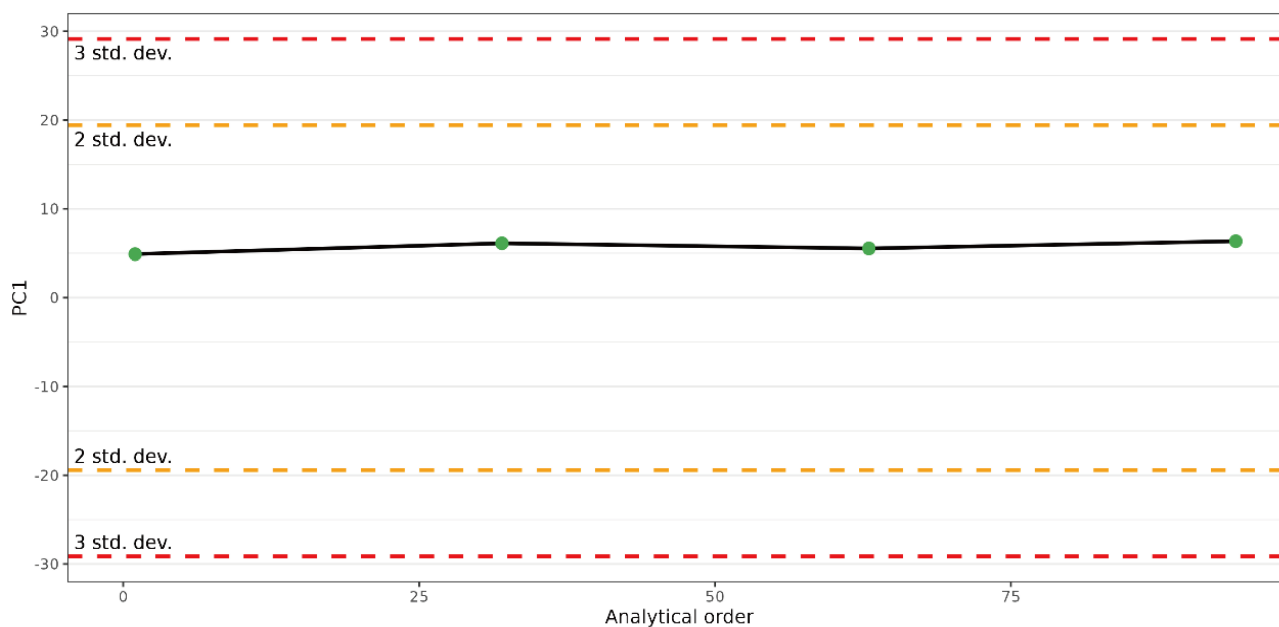
F I G U R E 2. Time series plot of principal component 1 during the analytical batch is shown, with PCA analysis performed using Pareto scaling. PCA, principal component analysis; PC1, principal component 1; std. dev, standard deviation.
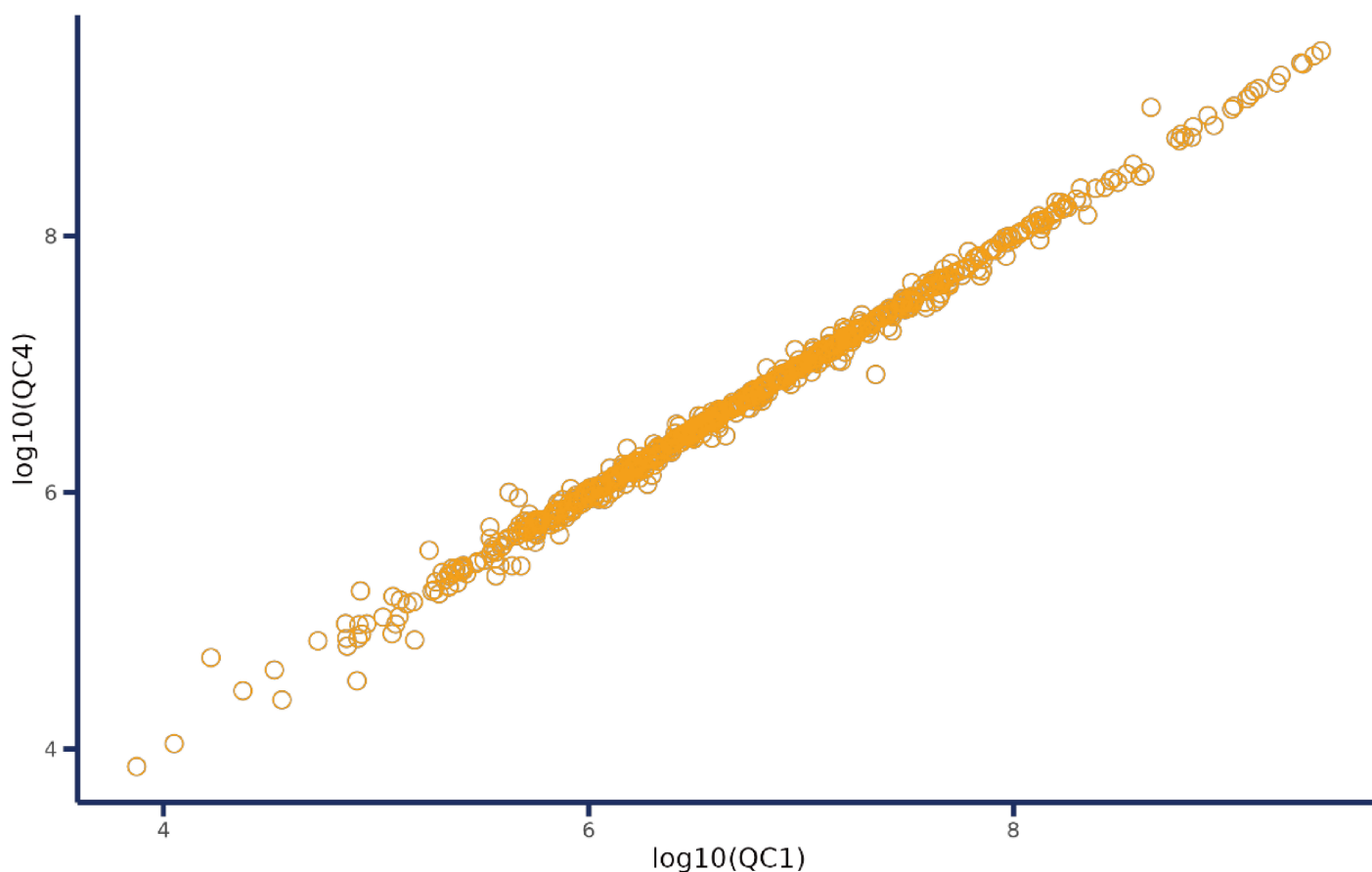
F I G U R E 3. First and last QC samples in the analytical batch showed a high correlation in Spearman correlation analysis, confirming the high quality of the acquired untargeted metabolomic data. QC, quality control.

ESI− mode.

In ESI+ mode, levels of hexenoylcarnitine (AcCa(6:1)) and lysophosphatidylcholine (LysoPC(20:5/0:0)) were significantly higher in PCa patients than in BPH patients, while phytosphingosine levels were lower. In ESI− mode, levels of (4E,15Z)-bilirubin IXa and bilirubin were elevated in PCa patients compared to BPH patients, while levels of C-mannosyl leucine and 3-hydroxymethylglutaric acid were significantly lower in PCa patients than in BPH patients. Overall, these results reveal significant metabolic differences between PCa and BPH.

Fig. 5 presents the ROC analysis results, demonstrating that these five key metabolites effectively differentiate BPH from PCa, with AUC values greater than 0.7 and p-values less than 0.05. Specifically, phytosphingosine (AUC = 0.703, sensitivity = 73.3%, specificity = 63.3%), LysoPC(0:0/20:4) (AUC = 0.722, sensitivity = 66.7%, specificity = 70.0%), (4E,15Z)-bilirubin IXa (AUC = 0.724, sensitivity = 86.7%, specificity = 53.3%), C-mannosyl leucine (AUC = 0.712, sensitivity = 73.3%, specificity = 63.3%), and dihydrothymine (AUC = 0.729, sensitivity = 70.0%, specificity = 70.0%) showed excellent performance in differentiating PCa from BPH.

In 5-fold cross-validation, we trained and compared the performance of SVM and logistic regression models, ultimately selecting logistic regression, which had an average ROC-AUC of 0.78. The final model achieved an AUC of 0.852, with a sensitivity of 80.0% and a specificity of 83.3%. These findings suggest that the metabolic panel of differential metabolites and their combination have strong diagnostic potential for distinguishing BPH from PCa.

3.4 Metabolomic profiling differences between prostatitis and PCa

PCA analysis showed no significant difference in sample distribution trends between patients with prostatitis and those with prostate cancer (PCa) (Fig. 6A). However, OPLS-DA clearly demonstrated a significant distinction between prostatitis and PCa patients (Fig. 6B). The R^2Y and Q^2 values for the OPLS-DA model were 0.709 and 0.166, respectively. VIP >1 and $p < 0.05$ were used to identify differentiating metabolites. After excluding exogenous metabolites, we used the LASSO regression algorithm to select 19 key metabolites (Table 3), including seven detected in ESI+ mode and 12 in ESI− mode. In ESI+ mode, N-acetylcadaverine levels were lower in prostatitis patients than in PCa patients. In ESI− mode, glycohyocholic acid and oxalic acid levels were higher in prostatitis patients, while palmitoleic acid (Free Fatty Acid (FFA(16:1))) levels were lower.

Fig. 7 shows the ROC analysis results, indicating that

A

B
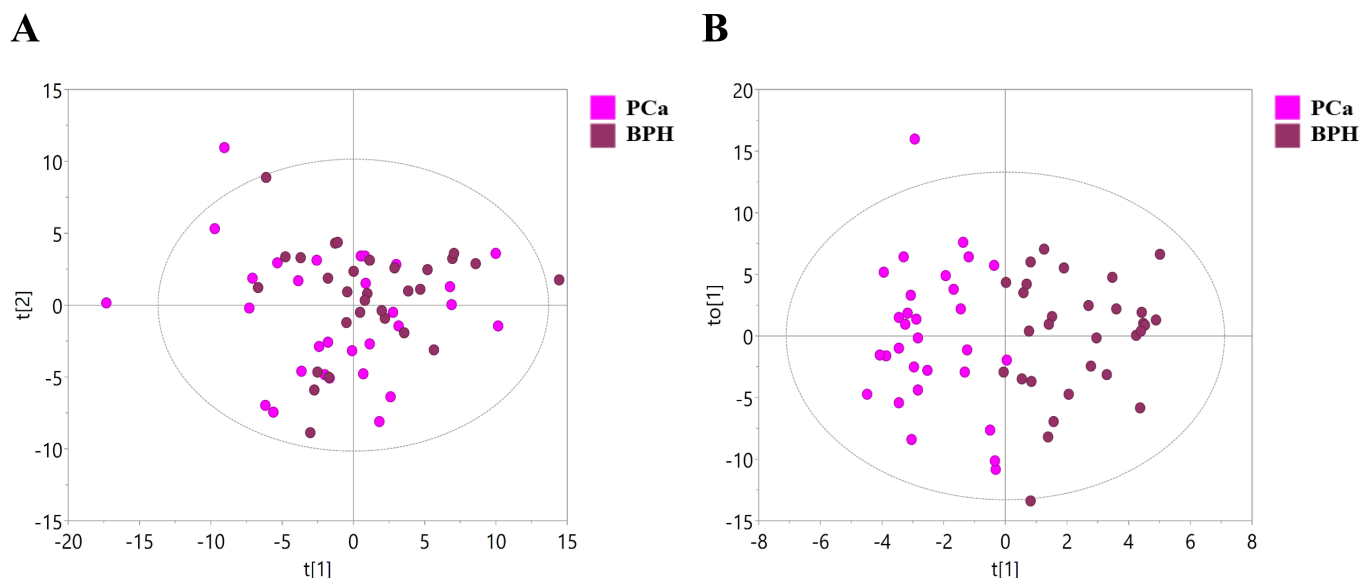
F I G U R E 4. PCA and OPLS-DA of LC-MS metabolite profiles of patients with PCa or BPH. (A) The PCA model's score scatter plot for patients with PCa and BPH is displayed. The X-axis represents the first principal component (t[1]), and the Y-axis represents the second principal component (t[2]). (B) The OPLS-DA model's score scatter plot for patients with PCa and BPH is displayed. The X-axis represents the predictive direction (t[1]), and the Y-axis represents the orthogonal direction (to[1]). Abbreviations: BPH, benign prostatic hyperplasia; LC-MS, liquid chromatography-mass spectrometry; PCa, prostate cancer; PCA, principal component analysis; OPLS-DA, orthogonal projections to latent structures-discriminate analysis.

T A B L E 2. Essential metabolites differentially expressed in patients with PCa and those with BPH.

Metabolite name	VIP	p-value	Fold change	Theoretical M/Z	AUC
Positive ion mode (ESI+)					
Dihydrothymine	1.26814	0.001105	1.2210	129.06585	0.729
Phytosphingosine	1.71774	0.002970	0.6409	318.30027	0.703
Hexenoylcarnitine (AcCa(6:1))	1.25281	0.014690	1.7700	258.16998	0.695
LysoPC(0:0/20:4)	1.24630	0.015860	1.3730	544.33977	0.722
LysoPC(20:5/0:0)	1.27482	0.019870	1.6950	542.32412	0.698
Ser-Leu	1.01905	0.031910	1.3110	219.13393	0.649
Negative ion mode (ESI−)					
(4E,15Z)-bilirubin IXa	1.92984	0.001121	1.9020	583.25621	0.724
C-mannosyl leucine	1.49497	0.007691	0.6862	292.14018	0.712
Bilirubin	1.45246	0.008296	1.3790	585.27076	0.690
3-Hydroxymethylglutaric acid	1.52828	0.022000	0.7060	161.04555	0.643
Ribonic acid + xylonate	1.09243	0.037240	0.8644	165.04046	0.662
Ascorbic acid-2-sulfate	1.02840	0.037280	0.8347	254.98163	0.684

Note. Fold change: PCa versus BPH. Abbreviations: BPH, benign prostatic hyperplasia; ESI, electrospray ionization; PCa, prostate cancer; VIP, variable importance in the projection; M/Z, mass-to-charge ratio; AUC, area under the curve.

the differentiation between prostatitis and PCa had an AUC greater than 0.7 and p-values less than 0.05. The eight key metabolites identified included pregnenolone sulfate (AUC = 0.724, sensitivity = 76.7%, specificity = 63.3%), bilirubin (AUC = 0.779, sensitivity = 76.7%, specificity = 76.7%), lysophosphatidylethanolamine (LysoPE(0:0/22:5n6)) + LysoPE(22:5n3/0:0) (AUC = 0.721, sensitivity = 63.3%, specificity = 70.0%), 5-hydroxyindole sulfate (AUC = 0.712, sensitivity = 66.7%, specificity = 80.0%), N-acetylcadaverine (AUC = 0.722, sensitivity = 50.0%, specificity = 83.3%), LysoPC(20:5/0:0) (AUC = 0.743, sensitivity = 73.3%, specificity = 76.7%), dihydrothymine (AUC = 0.749, sensitivity = 70.0%, specificity = 73.3%), and LysoPC(0:0/20:5) (AUC = 0.707, sensitivity = 63.3%, specificity = 76.7%). In 5-fold cross-validation, we trained and compared the performance of SVM and logistic regression models, ultimately selecting the SVM model, which achieved an average ROC-AUC of 0.867. The final model had an
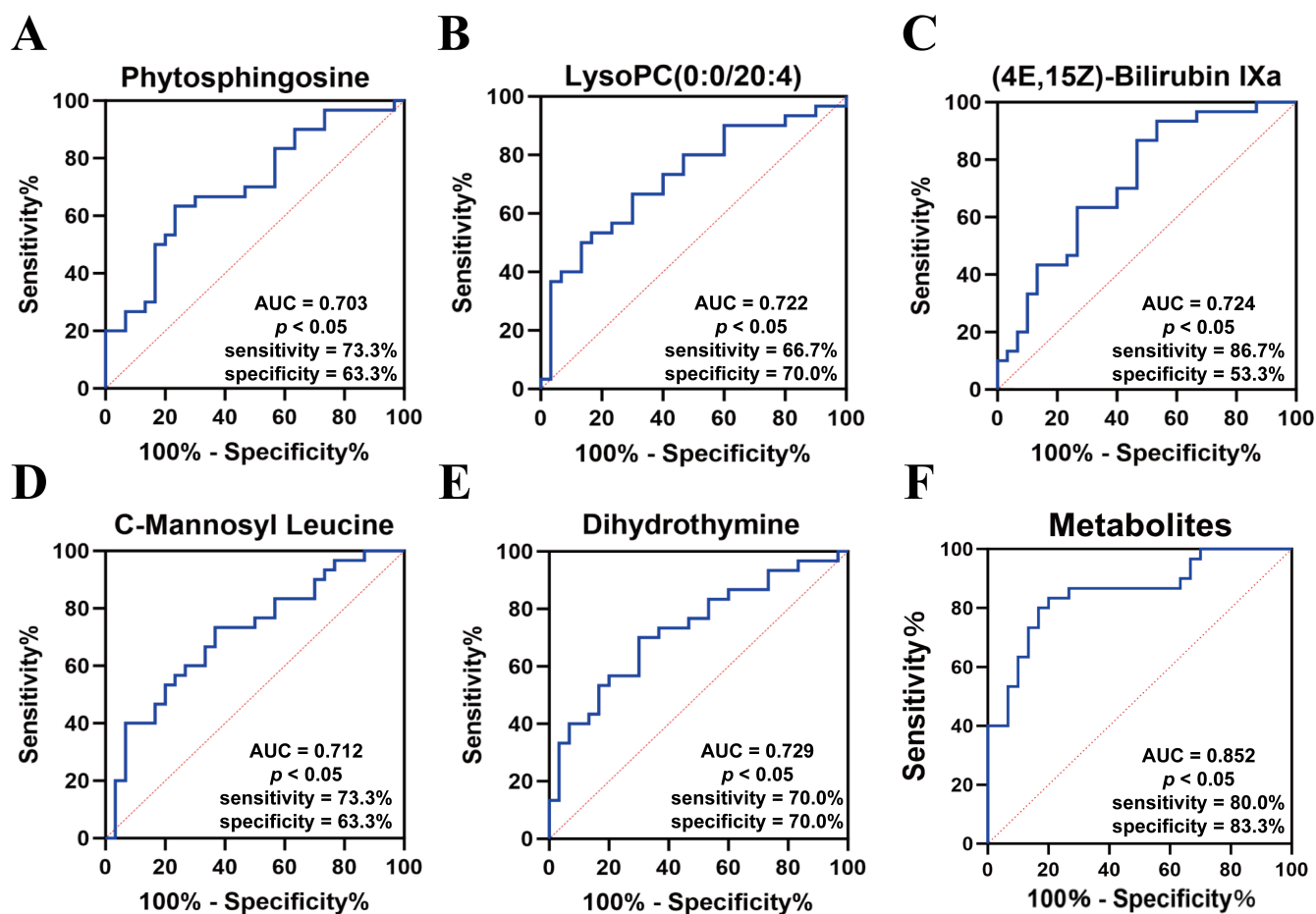
F I G U R E 5. ROC curve analysis of the selected essential metabolites for distinguishing PCa from BPH. Assessment of the diagnostic performance of phytosphingosine (A), LysoPC (0:0/20:4) (B), (4E,15Z)-bilirubin IXa (C), C-mannosyl leucine (D), dihydrothymine (E), and the combination of these six metabolites (F). Abbreviations: AUC, area under the ROC curve; BPH, benign prostatic hyperplasia; PCa, prostate cancer; ROC, receiver operating characteristic; LysoPC, lysophosphatidylcholine.
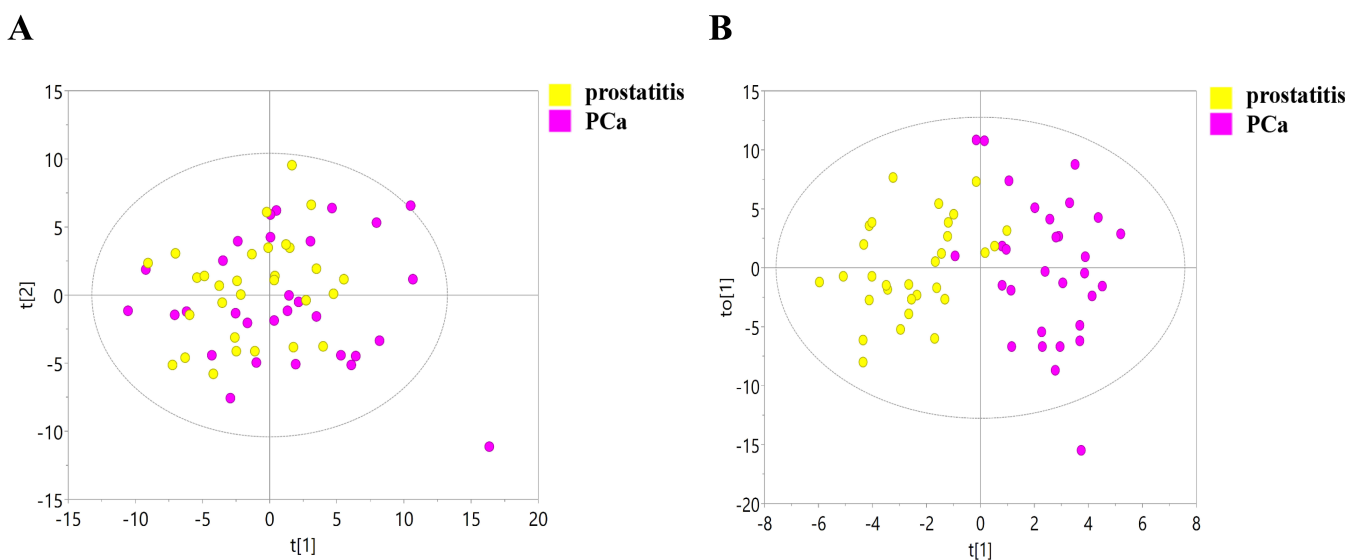
F I G U R E 6. PCA and OPLS-DA analyses of LC-MS metabolite profiles from patients with prostatitis and PCa. (A) Score scatter plot of the PCA model for patients with prostatitis and PCa. The X-axis represents the first principal component (t[1]), and the Y-axis represents the second principal component (t[2]). (B) Score scatter plot of the OPLS-DA model for patients with prostatitis and PCa. The X-axis represents the predictive direction (t[1]), and the Y-axis represents the orthogonal direction (to[1]). Abbreviations: LC-MS, liquid chromatography-mass spectrometry; PCa, prostate cancer; PCA, principal component analysis; OPLS-DA, orthogonal projections to latent structures-discriminate analysis.

T A B L E 3. Essential metabolites differentially expressed in patients with prostatitis and those with PCa.

Metabolite name	VIP	*p*-value	Fold change	Theoretical M/Z	AUC
Positive ion mode (ESI+)					
N-acetylcadaverine	1.41458	0.0009473	0.2987	145.13354	0.722
Dihydrothymine	1.25934	0.0014270	0.8149	129.06585	0.749
LysoPC(20:5/0:0)	1.63287	0.0025250	0.5383	542.32412	0.743
LysoPE(0:0/22:5n6) + lysoPE(22:5n3/0:0)	1.51744	0.0040010	0.6704	528.30847	0.721
LysoPC(0:0/20:5)	1.19229	0.0082190	0.6437	542.32412	0.707
Phytosphingosine	1.11388	0.0206700	0.5559	318.30027	0.649
LysoPE(22:6/0:0)	1.11551	0.0288400	0.7336	526.29282	0.677
Negative ion mode (ESI−)					
Bilirubin	1.66397	0.0001732	0.6433	585.27076	0.779
5-hydroxyindole sulfate	2.05320	0.0022320	0.5136	212.00230	0.712
Pregnenolone sulfate	1.47534	0.0031050	0.6668	395.18977	0.724
Pregnenolone-3,21-disulfate	1.22052	0.0069210	0.7424	245.06711	0.689
6-hydroxyindole sulfate	1.64359	0.0074630	0.5147	212.00230	0.673
Dehydroepiandrosterone sulfate	1.50858	0.0111700	0.7362	367.15847	0.696
Glycohyocholic acid	2.14660	0.0152300	1.4900	464.30176	0.698
M2X-RT295MZ165	1.93040	0.0195500	0.5873	165.09210	0.688
Palmitoleic acid (FFA(16:1))	2.34019	0.0201800	0.3921	253.21730	0.664
C-mannosyl leucine	1.38037	0.0217900	1.2900	292.14018	0.668
Oxalic acid	1.10862	0.0301200	1.4430	88.98803	0.687
M2X-RT307MZ165	1.52404	0.0492800	0.6162	165.09210	0.654

Note. Fold change: prostatitis versus PCa. Abbreviations: ESI, electrospray ionization; PCa, prostate cancer; VIP, variable importance in the projection; M/Z, mass-to-charge ratio; AUC, area under the curve; LysoPC, lysophosphatidylcholine; LysoPE, lysophosphatidylethanolamine; FFA, Free Fatty Acid.

AUC of 0.891, with a sensitivity of 76.7% and a specificity of 90.0%. These results indicate that the metabolic panel of differential metabolites and their combinations have strong diagnostic potential for distinguishing between prostatitis and PCa patients.

3.5 Metabolic pathway analysis of differential metabolites and construction of the metabolite-metabolite interaction network

Class analysis of the chemical properties of metabolites that differed between groups was conducted based on the structural annotation results from untargeted metabolomics with in-depth coverage (Fig. 8). A total of 712 metabolites were identified across 21 major classes, with 120 fatty acid species, accounting for 16.8% of the total. Metabolic phenotypes were then differentiated using PCA and OPLS-DA. Of the 109 differential metabolites identified in comparisons between prostatitis and PCa, fatty acid species were the most abundant, with 30 species. Fatty acid metabolites represented the largest proportion of all differential metabolites when comparing PCa and prostatitis patients. To explore the pathway-based metabolic features, we performed a metabolic pathway analysis on the differential metabolites (Fig. 9). Our find-

ings suggest that several metabolic pathways, including the biosynthesis of unsaturated fatty acids, play key roles in PCa. Additionally, the metabolite-metabolite interaction network (Fig. 10) highlighted hypoxanthine, oxalic acid, and succinic acid as central nodes for potential functional relationships among a wide range of annotated metabolites.

4. Discussion

Early diagnosis of PCa is crucial for improving patient survival. However, when PSA levels are in the range of 4–10 ng/mL, distinguishing between PCa, BPH and prostatitis becomes challenging, often leading to unnecessary biopsies. Therefore, there is an urgent need to explore new biomarkers to optimize clinical decision-making [20]. In this study, LC-MS-based untargeted metabolomics analysis revealed significant metabolic differences between patients with PCa, BPH and prostatitis. OPLS-DA showed distinct metabolic phenotypes among the three groups. Key metabolites, including fatty acids, phospholipids and bilirubin, were identified using LASSO regression, demonstrating potential diagnostic value in differentiating prostate diseases. In K-fold cross-validation, we trained and compared SVM and logistic regression models, evaluating their performance based on accuracy, precision, recall, F1-score and ROC-AUC. The best-performing model was
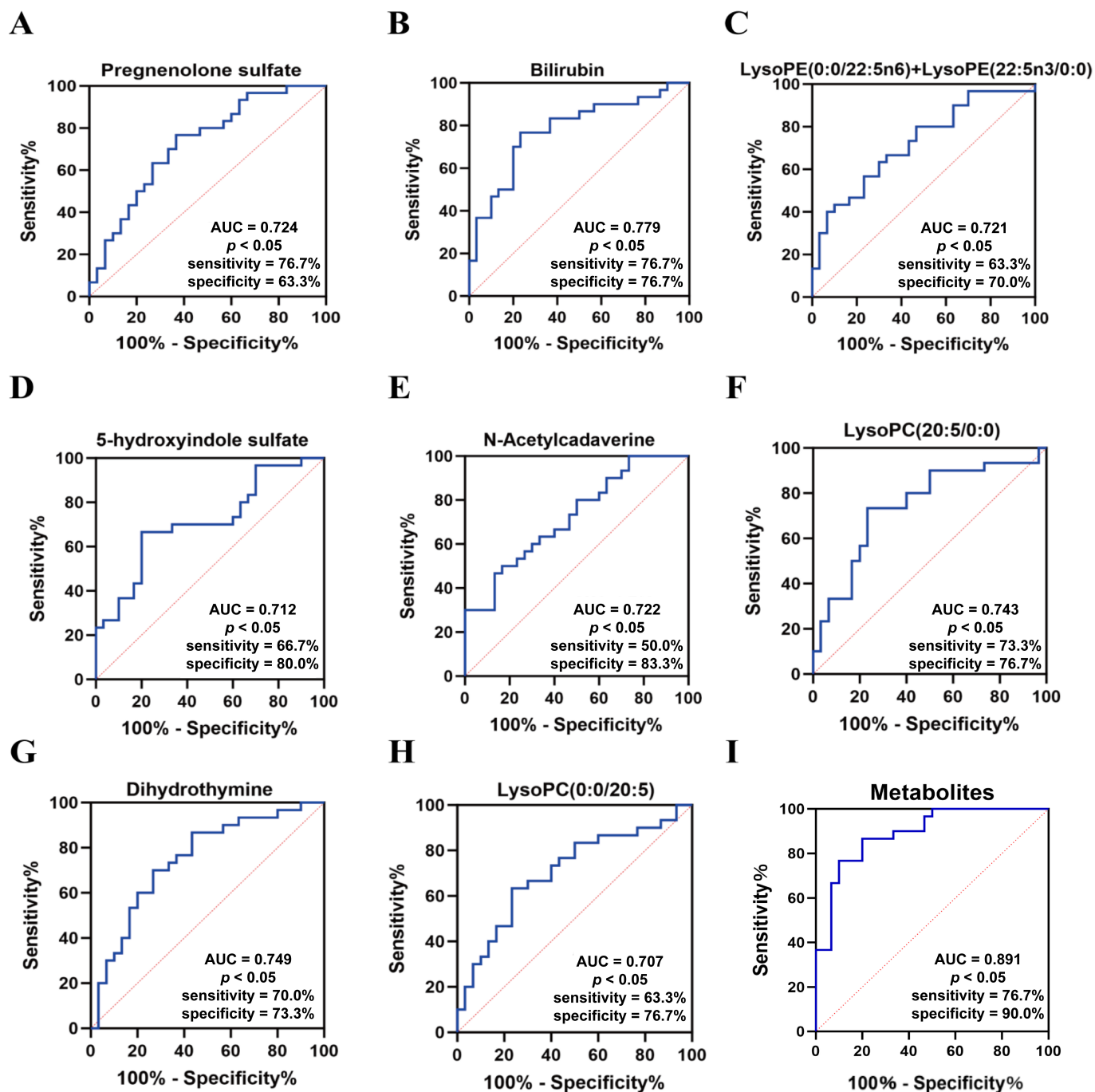
FIGURE 7. Displayed is the ROC curve analysis of the selected essential metabolites for distinguishing prostatitis from PCa. Assessment of the diagnostic performance of pregnenolone sulfate (A), bilirubin (B), LysoPE(0:0/22:5n6) + LysoPE(22:5n3/0:0) (C), 5-hydroxyindole sulfate (D), N-acetylcadaverine (E), LysoPC(20:5/0:0) (F), dihydrothymine (G), LysoPC(0:0/20:5) (H), and the combination of these eight metabolites (I). Abbreviations: AUC, area under the ROC curve; BPH, benign prostatic hyperplasia; PCa, prostate cancer; ROC, receiver operating characteristic; LysoPE, lysophosphatidylethanolamine; LysoPC, lysophosphatidylcholine.

selected and retrained on the entire dataset after the LASSO feature selection. The combination of multiple metabolites significantly improved the ability to distinguish PCa from BPH and prostatitis, with AUC values reaching 0.852 and 0.891, respectively. These results highlight the promising potential of metabolomics in the diagnosis of prostate diseases.

In recent years, metabolomics has garnered significant attention for its role in screening and early diagnosis of PCa. By analyzing metabolites in blood and urine samples, metabolomics can identify metabolic signatures associated with PCa, offering a precise tool for early detection [21]. This approach uncovers disease-related metabolic disruptions and is now widely recognized as a noninvasive diagnostic method [22, 23]. This study's PCA and OPLS-DA models revealed significant differences in the metabolic profiles of patients with PCa, BPH and prostatitis, particularly in pathways involving fatty acid, phospholipid, and sphingolipid metabolism. Key metabolites identified through LASSO regression included fatty acid metabo-
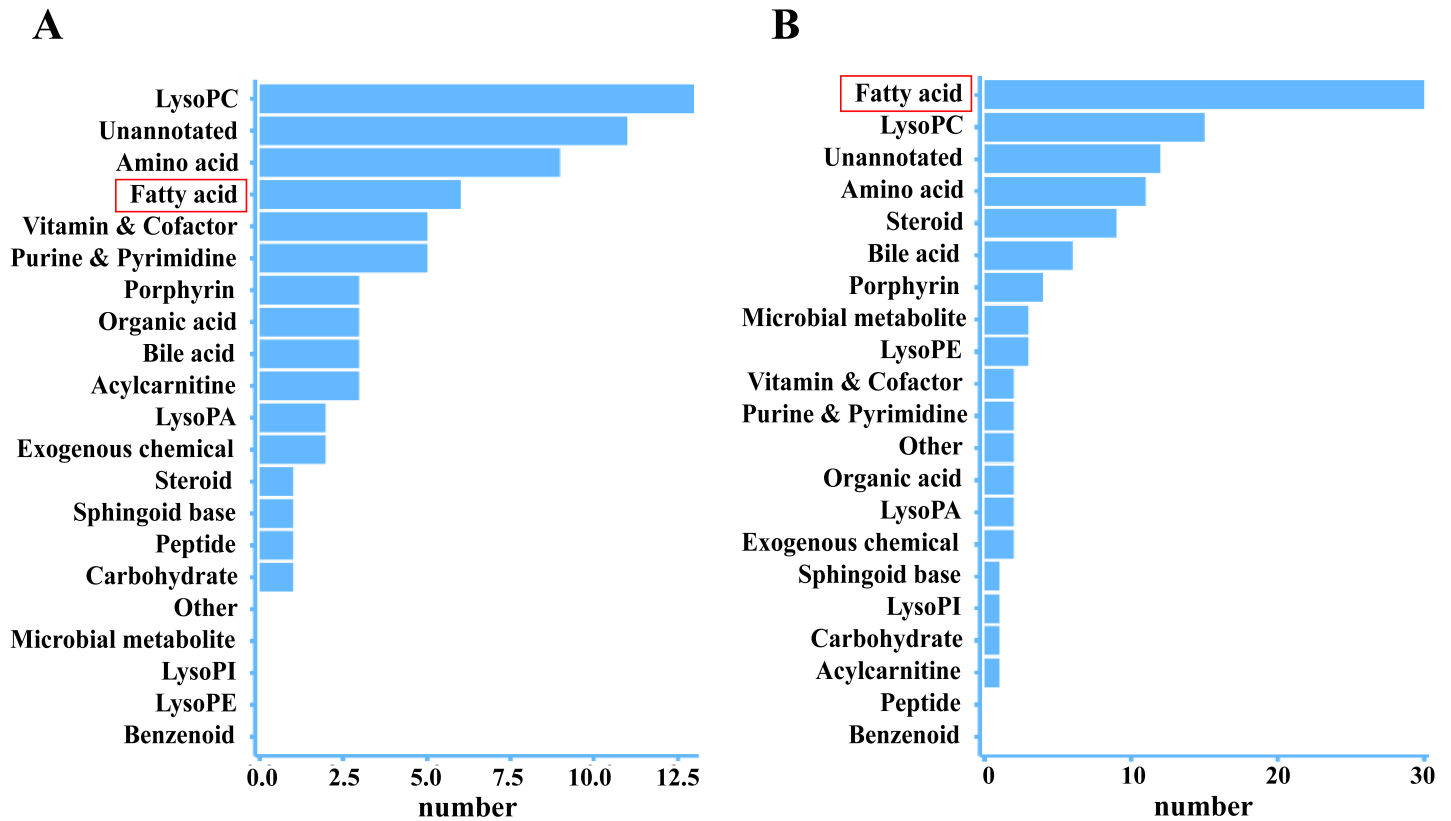
F I G U R E 8. Classification and quantification of significantly different metabolites (*p* < 0.05). (A) Differential metabolites in the comparison between PCa and BPH. (B) Differential metabolites in the comparison between PCa and prostatitis. The red boxes indicate that fatty acid metabolites represent a significantly larger proportion in both comparisons. Abbreviations: BPH, benign prostatic hyperplasia; PCa, prostate cancer; LysoPC, lysophosphatidylcholine; LysoPI, lysophosphatidylinositol; LysoPE, lysophosphatidylethanolamine; LysoPA, lysophosphatidic acid.
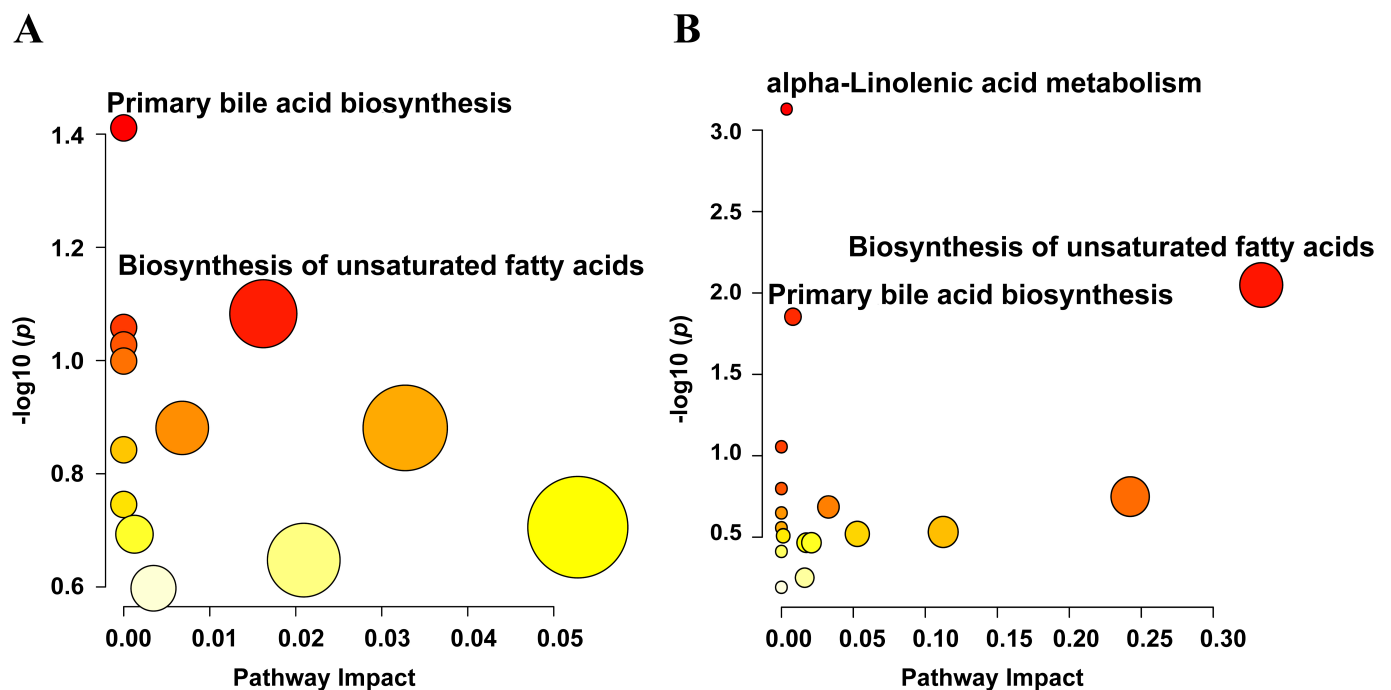
F I G U R E 9. The size of the bubbles is indicative of the pathway impacts, while the depth of the bubbles corresponds to the *p* value. (A) Pathway analysis with MetaboAnalyst of metabolites differing between PCa and BPH. (B) Pathway analysis with MetaboAnalyst of metabolites differing between PCa and prostatitis. Abbreviations: BPH, benign prostatic hyperplasia; PCa, prostate cancer.
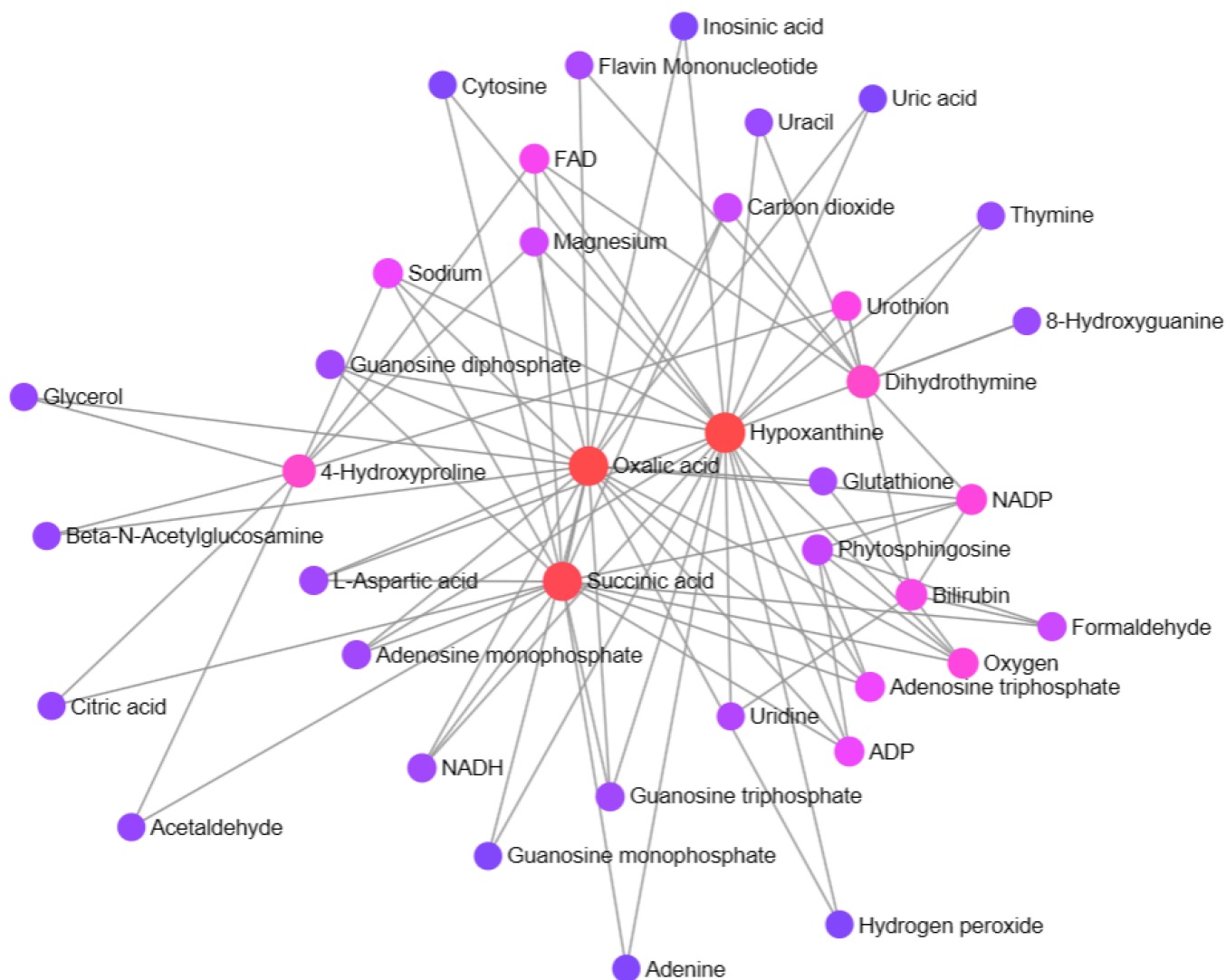
F I G U R E 1 0. **Construction of the metabolite interaction network reveals the metabolic processes in prostate cancer, highlighting the interactions between metabolites such as succinic acid and hypoxanthine.** FAD, flavin adenine dinucleotide; NADP, nicotinamide adenine dinucleotide phosphate; NADH, nicotinamide adenine dinucleotide (reduced); ADP, adenosine diphosphate.

lite hexenoylcarnitine and phospholipid metabolite LysoPC (20:5/0:0), which were significantly elevated in PCa patients. In contrast, the sphingolipid metabolite phytosphingosine was higher in BPH patients. These findings suggest a strong link between lipid metabolism and PCa progression.

A clinical study analyzing serum metabolites from 1812 Finnish men identified 49 metabolites linked to PCa-specific survival, including long-chain polyunsaturated fatty acids, phosphatidylcholine and glutamate. These metabolites were significantly correlated with a higher mortality risk in PCa patients [24]. Other studies have indicated that elevated levels of long-chain omega-3 polyunsaturated fatty acids are associated with a higher risk of prostate cancer, particularly high-grade cancers [25].

Metabolic reprogramming, a recognized hallmark of cancer, plays a crucial role in cancer cell proliferation, metastasis, and drug resistance [26]. Lipid metabolism reprogramming is considered a key driver in PCa development and progression since fatty acid metabolism is vital for energy storage, biomembrane

synthesis, and the production of tumor signaling molecules [27–29]. Research has demonstrated that overexpression of fatty acid synthase is linked to PCa aggressiveness and may serve as a crucial prognostic marker [30, 31]. Additionally, increased fatty acid uptake in PCa tissues has been confirmed, and targeting fatty acid uptake has been proposed as an effective therapeutic strategy [32–34].

In this study, ROC curve analysis identified key metabolites with AUC values ≥0.70. Among them, dihydrothymine demonstrated AUC values of 0.729 and 0.749, showing strong diagnostic capability in distinguishing PCa, BPH and prostatitis, with elevated levels of dihydrothymine found in PCa serum samples. Research has indicated that as a metabolic marker of thymine, abnormally high levels of dihydrothymine may induce cytotoxicity [35]. Combining multiple metabolites, such as phytosphingosine, bilirubin and dihydrothymine, further enhanced diagnostic sensitivity and specificity, with AUC values reaching 0.852 and 0.891. These results suggest that integrating metabolomic analyses of fatty acids, phospho-

lipids, and pyrimidine metabolites can significantly improve the accuracy of early PCa detection. Consistent with our findings, other researchers have also explored the value of serum organic acid metabolites in differentiating prostatitis, BPH and PCa. Their study revealed that organic acid metabolites detected through LC-MS can effectively distinguish between these prostate conditions, offering new possibilities for noninvasive early diagnosis [36]. Additionally, another study identified 18 lipid-related metabolites through serum metabolomic profiling. ROC curve analysis showed that these metabolites hold strong potential for differentiating PCa from BPH in patients within the PSA gray zone (4–10 ng/mL), with high diagnostic potential [37].

Metabolic pathway enrichment analysis revealed significant differences in several metabolic pathways between PCa, BPH and prostatitis, with unsaturated fatty acid biosynthesis, phospholipid metabolism, and pyrimidine metabolism being the key pathways. The elevation of unsaturated fatty acid metabolites in the serum of PCa patients underscores the pivotal role of fatty acid metabolism in tumor growth and proliferation. Studies have reviewed the role of polyunsaturated fatty acids (PUFA) in prostate cancer, showing that ω-6 PUFA is linked to PCa progression [27]. Additionally, phospholipid metabolite levels have been shown to effectively differentiate prostate cancer from benign prostatic hyperplasia [38]. The critical role of dihydrothymine in pyrimidine metabolism highlights the increased demand for DNA synthesis in PCa cells, as pyrimidine metabolism dysfunction has been closely linked to cancer progression [39]. Through metabolite interaction network analysis, metabolites such as hypoxanthine, oxalate, and succinate further illustrate the complexity of metabolic reprogramming in PCa. Notably, hypoxanthine-containing metabolites have been shown to effectively distinguish between BPH, prostate cancer, high-Gleason score PCa, and low-Gleason score PCa [40]. Furthermore, research has summarized the roles of tricarboxylic acid cycle metabolites in cancer, showing that metabolites such as hypoxanthine and succinate not only contribute to energy production but also drive tumor growth and spread by regulating epigenetics, cellular signaling, and redox balance [41].

5. Limitations

Several potential confounding factors may have influenced the observed metabolic profiles in this study. Despite participants fasting overnight, dietary habits prior to the study could still introduce variability, as high-fat or low-fat diets may impact lipid metabolism, particularly fatty acid metabolites. Physical activity levels may also play a role, as regular exercise is known to alter fatty acid metabolism, potentially affecting comparisons between PCa, BPH and prostatitis patients. Although participants who had used 5α-reductase inhibitors or medications affecting PSA levels were excluded, other medications, such as statins or anti-inflammatory drugs, may have influenced lipid and phospholipid metabolism. Comorbidities, including undiagnosed or milder conditions such as diabetes or cardiovascular diseases, could also affect metabolic pathways, despite excluding those with severe diseases. Additionally, age-related metabolic changes and hormonal fluctuations, par-

ticularly variations in testosterone levels, could act as confounding factors, even though the study population was limited to individuals over 50 years of age. These factors should be considered when interpreting the metabolic profiles observed in this study.

However, several limitations should be acknowledged. (1) Patients with prostatitis and BPH in this study did not undergo saturation biopsy; thus, there is a small possibility that some may have undiagnosed PCa. (2) Untargeted metabolomics does not provide precise quantification of metabolite abundance, necessitating further analysis of key metabolites using targeted metabolomic techniques. (3) While potential metabolic biomarkers were identified in serum samples, these findings need to be validated in other biofluids and matched tissue samples. (4) As this study was conducted at a single center with a relatively small sample size, validation in a larger multicenter cohort is required. (5) Metabolomics can be influenced by various factors, such as food intake, dietary habits and exercise, which were not controlled for in this study.

6. Conclusions

This study identified key metabolic biomarkers using LC-MS, achieving AUC values of 0.852 for PCa versus BPH and 0.891 for PCa versus prostatitis through LASSO regression and machine learning models. Fatty acid metabolism was a key feature of PCa. These findings suggest that a noninvasive metabolic biomarker panel could improve early PCa detection, particularly in the PSA gray zone, while reducing unnecessary biopsies. Validation in larger cohorts is still needed.

AVAILABILITY OF DATA AND MATERIALS

The data presented in this study are available on reasonable request from the corresponding author.

AUTHOR CONTRIBUTIONS

CW—contributed to the study design, drafted the manuscript. TC, SPH, YTP and TFG—performed the study. JL—revised the draft. All authors contributed to editorial changes in the manuscript. All authors read and approved the final manuscript.

ETHICS APPROVAL AND CONSENT TO PARTICIPATE

All participants were informed about the study, and written informed consent was obtained. The study was conducted in accordance with the criteria of the Declaration of Helsinki and was approved by the Ethics Committee of Lishui Central Hospital (Approval no: LSCHEC-2024-348).

ACKNOWLEDGMENT

Not applicable.

REFERENCES

[1] Zhang E, Chen Z, Liu W, Lin L, Wu L, Guan J, *et al*. NCAPG2 promotes prostate cancer malignancy and stemness via STAT3/c-MYC signaling. Journal of Translational Medicine. 2024; 22: 12.

[2] Ajiboye BO, Fatoki TH, Akinola OG, Ajeigbe KO, Bamisaye AF, Domínguez-Martín EM, *et al*. *In silico* exploration of anti-prostate cancer compounds from differential expressed genes. BMC Urology. 2024; 24: 138.

[3] Hu X, Liao J, Shan H, He H, Du Z, Guan M, *et al*. A novel carboxyl polymer-modified upconversion luminescent nanoprobe for detection of prostate-specific antigen in the clinical gray zonebase by flow immunoassay strip. Methods. 2023; 215: 10–16.

[4] Jue JS, Alameddine M. Role of PSA density and MRI in PSA interpretation. Comment on Lumbreras *et al*. variables associated with false-positive PSA results: a cohort study with real-world data. Cancers 2023, 15, 261. Cancers. 2023; 15: 2649.

[5] Flores-Fraile MC, Padilla-Fernández BY, Valverde-Martínez S, Marquez-Sanchez M, García-Cenador MB, Lorenzo-Gómez MF, *et al*. The association between prostate-specific antigen velocity (PSAV), value and acceleration, and of the free PSA/total PSA index or ratio, with prostate conditions. Journal of Clinical Medicine. 2020; 9: 3400.

[6] Abashidze N, Stecher C, Rosenkrantz AB, Duszak R III, Hughes DR. Racial and ethnic disparities in the use of prostate magnetic resonance imaging following an elevated prostate-specific antigen test. JAMA Network Open. 2021; 4: e2132388.

[7] Nordström T, Discacciati A, Bergman M, Clements M, Aly M, Annerstedt M, *et al*. Prostate cancer screening using a combination of risk-prediction, MRI, and targeted prostate biopsies (STHLM3-MRI): a prospective, population-based, randomised, open-label, non-inferiority trial. The Lancet Oncology. 2021; 22: 1240–1249.

[8] Grönberg H, Adolfsson J, Aly M, Nordström T, Wiklund P, Brandberg Y, *et al*. Prostate cancer screening in men aged 50–69 years (STHLM3): a prospective population-based diagnostic study. The Lancet Oncology. 2015; 16: 1667–1676.

[9] Eklund M, Jäderling F, Discacciati A, Bergman M, Annerstedt M, Aly M, *et al*. MRI-targeted or standard biopsy in prostate cancer screening. The New England Journal of Medicine. 2021; 385: 908–920.

[10] Wang Q, Ding L, Wang R, Liang Z. A review on the morphology, cultivation, identification, phytochemistry, and pharmacology of *Kitagawia praeruptora* (Dunn) Pimenov. Molecules. 2023; 28: 8153.

[11] Wang H, Yin Y, Zhu ZJ. Encoding LC-MS-based untargeted metabolomics data into images toward AI-based clinical diagnosis. Analytical Chemistry. 2023; 95: 6533–6541.

[12] Nie M, Yao K, Zhu X, Chen N, Xiao N, Wang Y, *et al*. Evolutionary metabolic landscape from preneoplasia to invasive lung adenocarcinoma. Nature Communications. 2021; 12: 6479.

[13] Bondar OP, Barnidge DR, Klee EW, Davis BJ, Klee GG. LC-MS/MS quantification of Zn-alpha2 glycoprotein: a potential serum biomarker for prostate cancer. Clinical Chemistry. 2007; 53: 673–678.

[14] Moses KA, Sprenkle PC, Bahler C, Box G, Carlsson SV, Catalona WJ, *et al*. NCCN Guidelines® insights: prostate cancer early detection, version 1.2023. Journal of the National Comprehensive Cancer Network. 2023; 21: 236–246.

[15] Murthy DP, Ray U, Morewaya J, SenGupta SK. A study of the correlation of prostatic pathology and serum prostate-specific antigen (PSA) levels: a perspective from Papua New Guinea. Papua New Guinea Medical Journal. 1998; 41: 59–64.

[16] Wishart DS, Guo A, Oler E, Wang F, Anjum A, Peters H, *et al*. HMDB 5.0: the human metabolome database for 2022. Nucleic Acids Research. 2022; 50: D622–D631.

[17] Fan S, Kind T, Cajka T, Hazen SL, Tang WHW, Kaddurah-Daouk R, *et al*. Systematic error removal using random forest for normalizing large-scale untargeted lipidomics data. Analytical Chemistry. 2019; 91: 3590–3596.

[18] Barupal DK, Fiehn O. Chemical Similarity Enrichment Analysis (Chem-RICH) as alternative to biochemical pathway mapping for metabolomic datasets. Scientific Reports. 2017; 7: 14567.

[19] Pang Z, Zhou G, Ewald J, Chang L, Hacariz O, Basu N, *et al*. Using MetaboAnalyst 5.0 for LC-HRMS spectra processing, multi-omics integration and covariate adjustment of global metabolomics data. Nature Protocols. 2022; 17: 1735–1761.

[20] Yang J, Li J, Xiao L, Zhou M, Fang Z, Cai Y, *et al*. ^{68}Ga-PSMA PET/CT-based multivariate model for highly accurate and noninvasive diagnosis of clinically significant prostate cancer in the PSA gray zone. Cancer Imaging. 2023; 23: 81.

[21] AlZaim I, Al-Saidi A, Hammoud SH, Darwiche N, Al-Dhaheri Y, Eid AH, *et al*. Thromboinflammatory processes at the nexus of metabolic dysfunction and prostate cancer: the emerging role of periprostatic adipose tissue. Cancers. 2022; 14: 1679.

[22] Cerrato A, Bedia C, Capriotti AL, Cavaliere C, Gentile V, Maggi M, *et al.* Untargeted metabolomics of prostate cancer zwitterionic and positively charged compounds in urine. Analytica Chimica Acta. 2021; 1158: 338381.

[23] Messina E, La Torre G, Pecoraro M, Pisciotti ML, Sciarra A, Poscia R, *et al*. Design of a magnetic resonance imaging-based screening program for early diagnosis of prostate cancer: preliminary results of a randomized controlled trial—Prostate Cancer Secondary Screening in Sapienza (PROSA). European Radiology. 2024; 34: 204–213.

[24] Huang J, Zhao B, Weinstein SJ, Albanes D, Mondul AM. Metabolomic profile of prostate cancer-specific survival among 1812 Finnish men. BMC Medicine. 2022; 20: 362.

[25] Farrell SW, DeFina LF, Tintle NL, Leonard D, Cooper KH, Barlow CE, *et al.* Association of the omega-3 index with incident prostate cancer with updated meta-analysis: the cooper center longitudinal study. Nutrients. 2021; 13: 384.

[26] Faubert B, Solmonson A, DeBerardinis RJ. Metabolic reprogramming and cancer progression. Science. 2020; 368: eaaw5473.

[27] Liu B, Liu C, Chai X, Fan X, Huang T, Zhan J, *et al*. Real-time NMR-based drug discovery to identify inhibitors against fatty acid synthesis in living cancer cells. Analytical Chemistry. 2024; 96: 3034–3043.

[28] Zhang FB, Gan L, Zhu TH, Ding HQ, Wu CH, Guan YT, *et al*. Pan-cancer analyses reveal genomics and clinical outcome association of the fatty acid oxidation regulators in cancer. Heliyon. 2024; 10: e28441.

[29] Berquin IM, Edwards IJ, Kridel SJ, Chen YQ. Polyunsaturated fatty acid metabolism in prostate cancer. Cancer and Metastasis Reviews. 2011; 30: 295–309.

[30] Cao Z, Xu Y, Guo F, Chen X, Ji J, Xu H, *et al*. FASN Protein overexpression indicates poor biochemical recurrence-free survival in prostate cancer. Disease Markers. 2020; 2020: 3904947.

[31] Dłubek J, Rysz J, Jabłonowski Z, Gluba-Brzózka A, Franczyk B. The correlation between lipid metabolism disorders and prostate cancer. Current Medicinal Chemistry. 2021; 28: 2048–2061.

[32] Watt MJ, Clark AK, Selth LA, Haynes VR, Lister N, Rebello R, *et al.* Suppressing fatty acid uptake has therapeutic effects in preclinical models of prostate cancer. Science Translational Medicine. 2019; 11: eaau5758.

[33] Sena LA, Denmeade SR. Fatty acid synthesis in prostate cancer: vulnerability or epiphenomenon? Cancer Research. 2021; 81: 4385–4393.

[34] Galbraith L, Leung HY, Ahmad I. Lipid pathway deregulation in advanced prostate cancer. Pharmacological Research. 2018; 131: 177–184.

[35] Mukherjee S, Papadopoulos D, Chari N, Ellis D, Charitopoulos K, Charitopoulos I, *et al*. High-grade prostate cancer demonstrates preferential growth in the cranio-caudal axis and provides discrimination of disease grade in an MRI parametric model. British Journal of Radiology. 2024; 97: 574–582.

[36] Lovegrove CE, Matanhelia M, Randeva J, Eldred-Evans D, Tam H, Miah S, *et al*. Prostate imaging features that indicate benign or malignant pathology on biopsy. Translational Andrology and Urology. 2018; 7:

S420–S435.

[37] Lee CM, Park KJ, Kim MH, Kim JK. Ancillary imaging and clinical features for the characterization of prostate lesions: a proposed approach to reduce false positives. Journal of Magnetic Resonance Imaging. 2021; 53: 1887–1897.

[38] Parmar C, Barry JD, Hosny A, Quackenbush J, Aerts HJWL. Data analysis strategies in medical imaging. Clinical Cancer Research. 2018; 24: 3492–3499.

[39] Kuzudisli C, Bakir-Gungor B, Bulut N, Qaqish B, Yousef M. Review of feature selection approaches based on grouping of features. PeerJ. 2023; 11: e15666.

[40] Remeseiro B, Bolon-Canedo V. A review of feature selection methods in medical applications. Computers in Biology and Medicine. 2019; 112: 103375.

[41] McNitt-Gray M, Napel S, Jaggi A, Mattonen SA, Hadjiiski L, Muzi M, *et al*. Standardization in quantitative imaging: a multicenter comparison of radiomic features from different software packages on digital reference objects and patient data sets. Tomography. 2020; 6: 118–128.